MINERALISATION IN ORE ZONE 1, MILIN KAMAK DEPOSIT, WESTERN SREDNOGORIE, BULGARIA

Daniela Nikolova, Sergey Dobrev, Kalin Ruskov

University of Mining and Geology "St. Ivan Rilski", 1700 Sofia; danny.nikolova@abv.bg

ABSTRACT. The Milin Kamak deposit is located in the Western Srednogorie zone. This zone is part of the Late Cretaceous Apuseni-Banat-Timok-Srednogorie magmatic and metallogenic belt. The mineralisation is gold-silver, epithermal, intermediate sulfidation type. The deposit represents a product of the Breznik paleovolcano. Ore mineralisation is formed in three stages: quartz-pyrite, quartz-polymetallic and carbonate-gold. In this study mineral composition of Ore Zone 1 is discussed, represented by pyrite, marcasite, arsenopyrite, chalcopyrite, galena, sphalerite, tennantite-tetrahedrite, enargite, bornite, covellite, hematite, pyrrhotite, seligmanite-bournonite, jordanite (?), robinsonite (?) and native gold. The gangue minerals are represented by quartz, carbonates and barite.

Keywords: Late Cretaceous, Western Srednogorie, Milin Kamak, ore zone 1, ore minerals

МИНЕРАЛИЗАЦИЯ НА РУДНА ЗОНА 1, НАХОДИЩЕ "МИЛИН КАМЪК", ЗАПАДНО СРЕНОГОРИЕ, БЪЛГАРИЯ

Даниела Николова, Сергей Добрев, Калин Русков

Минно-геоложки университет "Св. Иван Рилски", 1700 София

РЕЗЮМЕ. Находище "Милин камък" се намира в Западното Средногорие. Тази зона е част от къснокредния Апусени-Банат-Тимок-Средногорски магматичен и металогенен пояс. Минерализацията е златно-сребърна, епитермална, от умереносулфиден тип. Находището е продукт на Брезнишкия палеовулкан. Рудната минерализация е отложена в три стадия: кварц-пиритов, кварц-полиметален и карбонатно-златен. Разгледан е минералният състав на рудна зона 1, представен от пирит, марказит, арсенопирит, халкопирит, галенит, сфалерит, тенантит-тетраедрит, енаргит, борнит, ковелин, хематит, пиротин, селигманит-бурнонит, йорданит (?), робинсонит (?) и самородно злато. От нерудните минерали присъстват кварц, карбонати и барит.

Ключови думи: Късна Креда, Западно Средногорие, Милин Камък, рудна зона 1, рудни минерали

Geological settings of the Milin Kamak deposit

The Milin Kamak deposit is situated in the Sofia tectonic unit in the western part of the Srednogorie Zone of Apuseni-Banat-Timok-Srednogorie magmatic and metallogenic belt (Popov et al., 2002). It is located in propylitic, sericitic and argillic altered Late Cretaceous trachybasalt to andesitic volcanic and volcanoclastic rocks (Dabovski et al., 2009) – products of Breznic paleo-vulcano (Fig. 1). A part of the sequence is overlain by Paleogene and Neogene sediments. To the south-west, Permian to Jurassic sequence of continental to marine sediments, represented by sandstones, clay and limestone, is observed.

The gold-silver epitermal deposit Milin Kamak is situated south-west from the Krasava syncline. The major faults and shear zones are with N-W orientation, parallel to the paleo-subduction line (oceanic crust beneath the Eurasian continental margin – Dabovski et al., 2009). Later formed faults with NE direction are cross-cutting former ones. E-W striking secondary faults host the ore mineralisation.

The Ore Zone 1 is a vein with numerous apophyses. The ore body is with E-W orientation, dipping steeply to the south. It is located within intensively brecciated rocks and is considered to be the most promising part of the deposit.

Material and methods

For the purpose of this study 30 representative samples from drill holes and adits have been taken. All the samples are with visible ore mineralisation and high gold content. Position of samples (polished sections respectively) at level 760 m is given in Figure 2. Polished sections were investigated at the University of Mining and Geology "St. Ivan Rilski" (UMG) under reflected plane polarised light with microscope Meiji MT-9430. Microphotographs were taken with a digital camera Meiji Infinity-1 and a reflex digital photo camera Nikon D3200, mounted on a trinocular. Electron microprobe analyses of ore minerals have been done using X-ray spectral micro analyser JEOL JSM-6010 PLUS LA, with EDS spectrometer at the UMG "St. Ivan Rilski". The mode of operation is determined by the following analytical conditions: 20 kV accelerating voltage, 30 Pa pressure and High vacuum. The standards used are pure metal Cu and Al.

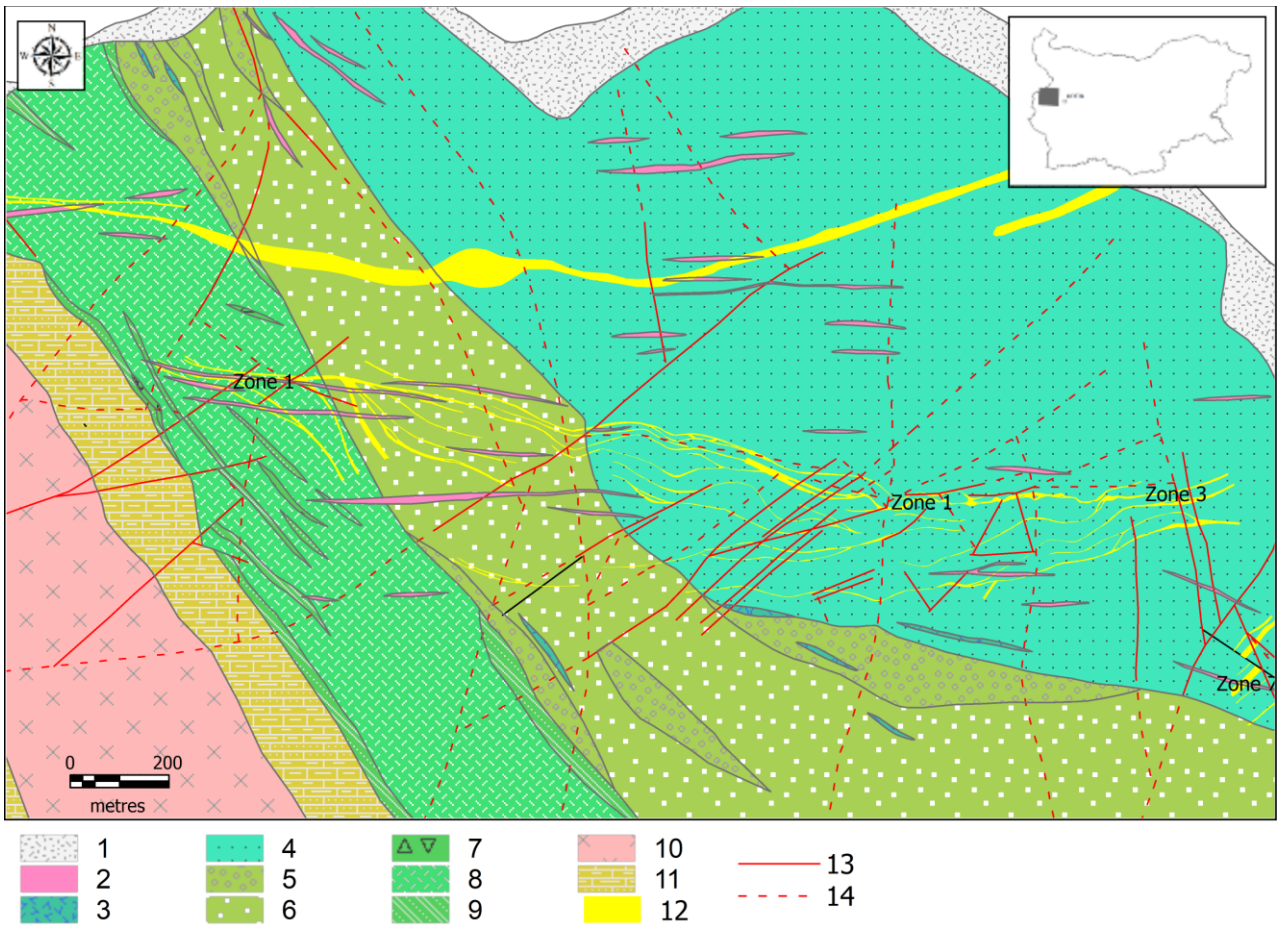

Fig. 1. Geological map of the Milin Kamak deposit and Ore Zones (data from "Thrace Resources" Ltd)
1, alluvial sediments; *2*, andesitobasalt dyke; *3*, basalt and andesitobasalt lavas; *4*, agglomerate tuffs; *5*, bomb–block tuffs; *6*, lapilli–psephitic tuffs; *7*, trachybasalt lavas; *8*, lapilli tuffs; *9*, beds of psephytic and pellitic tuffs; *10*, trachyandesites (plagioclase); *11*, sediment alternation; *12*, ore zone; *13*, certain fault; *14*, supposed fault

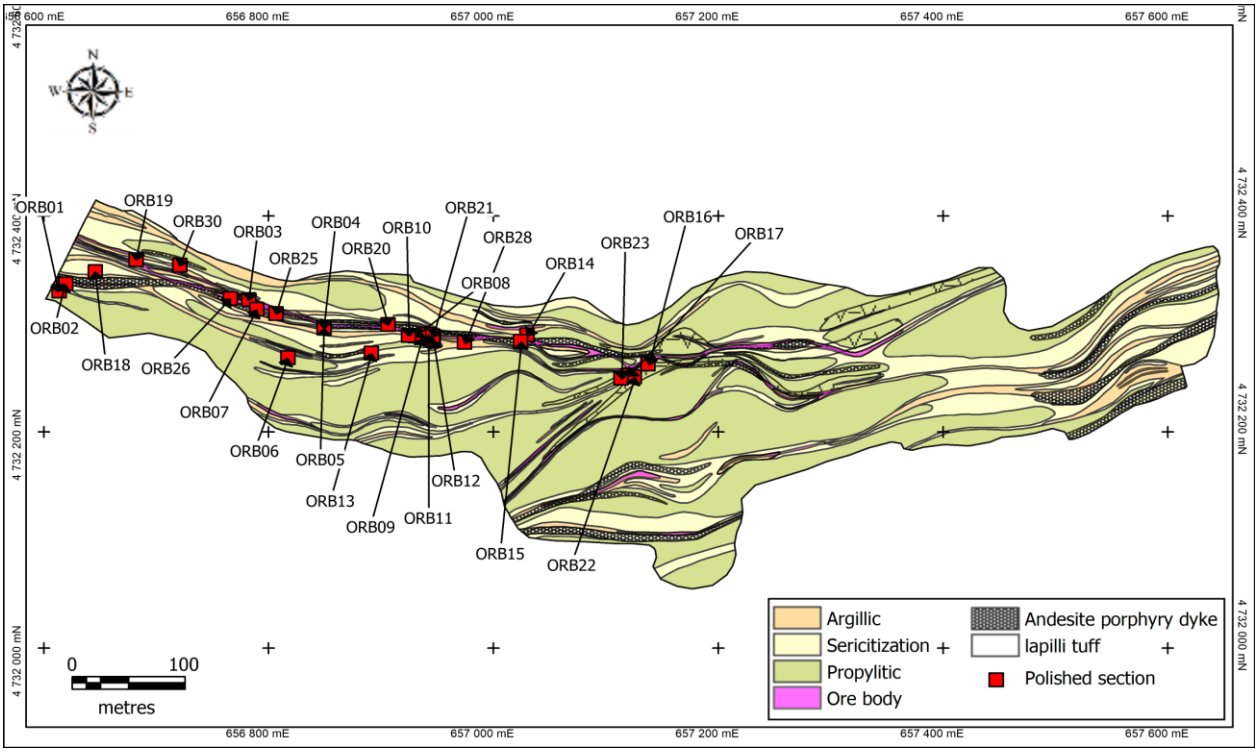

Fig. 2. Plan of level 760 with different types of alteration and position of samples (polished sections) in Ore Zone 1, Milin Kamak deposit (data from "Thrace Resources" Ltd.)

Mineralogy

Ore minerals

Pyrite is the main ore mineral. It appears as aggregates with xenomorphic to semi-euhedral shape (Fig. 3.F, 3.J) and size less than 100 μm (Fig. 3.B), in some cases with colloform structure ("melnikovite-pyrite"). It is often observed as large irregular grains with bay-like contours (Fig. 3.G), rarely as euhedral (Fig. 3.B) and subhedral grains, often with zonal structure. In larger grains inclusions from galena, chalcopyrite, sphalerite, pyrrhotite and tennantite-tetrahedrite (Fig. 3.H) are present. Pyrite appears as aggregates with irregular shape and sometimes with skeleton contours intensively corroded by carbonates. In some cases it associates with marcasite (Fig. 3.A). Single electron microprobe analysis determines content of As 1.69 wt% comparatively lower than reported by Stoykov et al. (2007). The calculated formula is $(Fe_{1.02}As_{0.03})_{1.05}S_{1.95}$ (Table 1).

Marcasite is the second by distribution ore mineral. It usually forms fine veinlets, platy and elongated prismatic to needle-like grains often in characteristic star-like aggregates (Fig. 3.J). Marcasite crystals with platy to prismatic habit often are rimming large pyrite aggregates (Fig. 3.A). Marcasite forms aggregates with mosaic structure together with pyrite in association with chalcopyrite, sphalerite and galena. Usually it forms fine-grained aggregates with a woody or colloform structure. Marcasite is observed as fine-grained strips among Mn-calcite with banded structure. In some cases it associates with chalcopyrite and sphalerite rimming large tennantite-tetrahedrite grains (Fig. 3.C). It demonstrates distinct bireflectance and strong anisotropy with colour effects from blue-green to dark brown. No impurities were determined with calculated formulas $Fe_{1.03}S_{1.98}$ and $Fe_{1.04}S_{1.95}$ (Table 1).

Arsenopyrite is rarely observed in rhombic shaped crystals and "larkspur" intergrowths (Fig. 3.B) or star-like aggregates. Arsenopyrite is characterised by high reflectance, white colour and strong anisotropy with colour effects (bluish to yellow-brown). The formulas based on microprobe analyses are $Fe_{1.04}As_{0.86}S_{1.09}$, $Fe_{1.04}As_{0.85}S_{1.11}$, $Fe_{1.05}As_{0.83}S_{1.12}$ (Table 1).

Chalcopyrite is established as emulsion within sphalerite grains and inclusions with size less than 20 μm in quartz, pyrite, marcasite (Fig. 3.C, 3.H), galena and sphalerite (Fig. 3.K). Together with marcasite, it forms a rim around sphalerite or pyrite grains and cross-cutting the latter ones in fine veinlets (Fig. 3.E). It is also observed as small grains within Mn-calcite. Chalcopyrite often forms joint aggregates with minerals from tennantite-tetrahedrite series (Fig. 3.E).

Galena also appears as individual grains with size up to 150 μm in peripheral parts of quartz veinlets. It is observed as euhedral crystals in sphalerite or corrodes pyrite grains as anhedral aggregates (Fig. 3.F). Galena is usually corroded by carbonates and barite. It often is observed together with bournonite-seligmannite and is overgrown by the latter one (Fig. 3.K). Microprobe analyses of two galena grains determine formulas $(Pb_{1.03}Sb_{0.04}Ag_{0.01})_{1.08}S_{0.92}$ and $Pb_{1.08}S_{0.92}$ (Table 1).

Sphalerite appears as coarse grains (from 3–4 mm to до 5–6 mm) with irregular shape (Fig. 3.C), often with rim from chalcopyrite and marcasite (Fig. 3.E). It appears as small inclusions in pyrite and forms aggregates with pyrite and marcasite, or with chalcopyrite, galena and mineral from tennantite-tetrahedrite series. Inclusions from pyrite are often observed, but chalcopyrite emulsion is not typical. Sphalerite is confirmed by single microprobe analysis – absence of iron (Table 1) and formula $Zn_{0.98}S_{1.02}$. It could be determined as cleiophane – manifests very intensive yellowish-brown internal reflections, often with well expressed zonal structure (Fig. 3.D).

Tennantite-tetrahedrite. A mineral from this series is found comparatively rare. It forms individual grains with large inclusions from chalcopyrite and smaller from galena and sphalerite. Such grains are often rimmed by fine-grained marcasite aggregates (Fig. 3.C). The mineral from tennantite-tetrahedrite series often associates with sulfides (chalcopyrite, sphalerite, galena and marcasite) and some sulfosalts (bournonite), filling interstitial spaces between large cracked pyrite grains in some cases accompanied by native gold (Fig. 3.J). Mainly As varieties have been determined, but also pure Sb members are present (Table 2). The latter ones are brighter in backscattered electrons. Microprobe analyses taken on different in brightness image from tennantite-tetrahedrite grain determines two end members of the series (Table 2) – mainly As (Zn-tennantite) $(Cu_{10.45}Zn_{1.69})_{12.14}(As_{2.63}Sb_{1.41})_{4.04}S_{12.82}$, and Sb – Ag-bearing Zn-tetrahedrite – $(Cu_{8.11}Ag_{2.40}Zn_{1.77})_{12.28}Sb_{4.07}S_{12.65}$. The composition of tennantite-tetrahedrite is similar to the theoretical, with a negligible S deficiency (Table 4).

Enargite. Among massive galena, a single grain from a grey mineral with distinct anisotropy was observed (Fig. 3.F). Microprobe analysis proves enargite (Table 3) with calculated formula $Cu_{3.04}As_{0.96}S_{4.00}$.

Bornite was found as single rounded inclusions within a pyrite grain. It did not manifest anisotropy and is characterised by a pink colour with brown shade. Presence of a chalcopyrite grain at the same photo suggests that bornite is an ore mineral with a primary origin.

Covellite is observed as inclusion together with minerals from tennantite-tetrahedrite series only in one pyrite grain (Fig. 3.G). The latter one is with indigo blue colour, shows strong bireflectance and pleochroism (to pale blue) and very strong anisotropy with colour effects (purple-red). No doubt it is an alteration product over chalcopyrite in the zone of secondary copper enrichment of the deposit.

Hematite was found as elongated prismatic inclusions with size up to 25 μm in just one pyrite grain associating with marcasite and sphalerite. Hematite grains manifest distinct anisotropy and in the largest one red internal reflection could be observed.

Pyrrhotite is observed as rounded drop-like inclusions with size up to 10 μm in some pyrite grains and is characterised by creamy colour and distinct anisotropy (Fig. 3.H).

Seligmannite-bournonite series mineral is often found as prismatic grains among gangue, observed at the periphery of galena grains or as separate individuals in close vicinity to galena grains, sphalerite, chalcopyrite and marcasite. They manifest distinct anisotropy and usually are with well expressed lamellar structure (Fig. 3.I). Colour in reflected light is light grey with reflection lower than that of galena. Minerals from seligmannite-bournonite series associates closely with other sulfosalt and late gangue minerals like barite and dolomite, often accompanied by native gold. Microprobe analyses determine mostly As varieties (seligmannite) but also pure bournonite presents (Table 3). The calculated formulas are with non-stoichiometric composition.

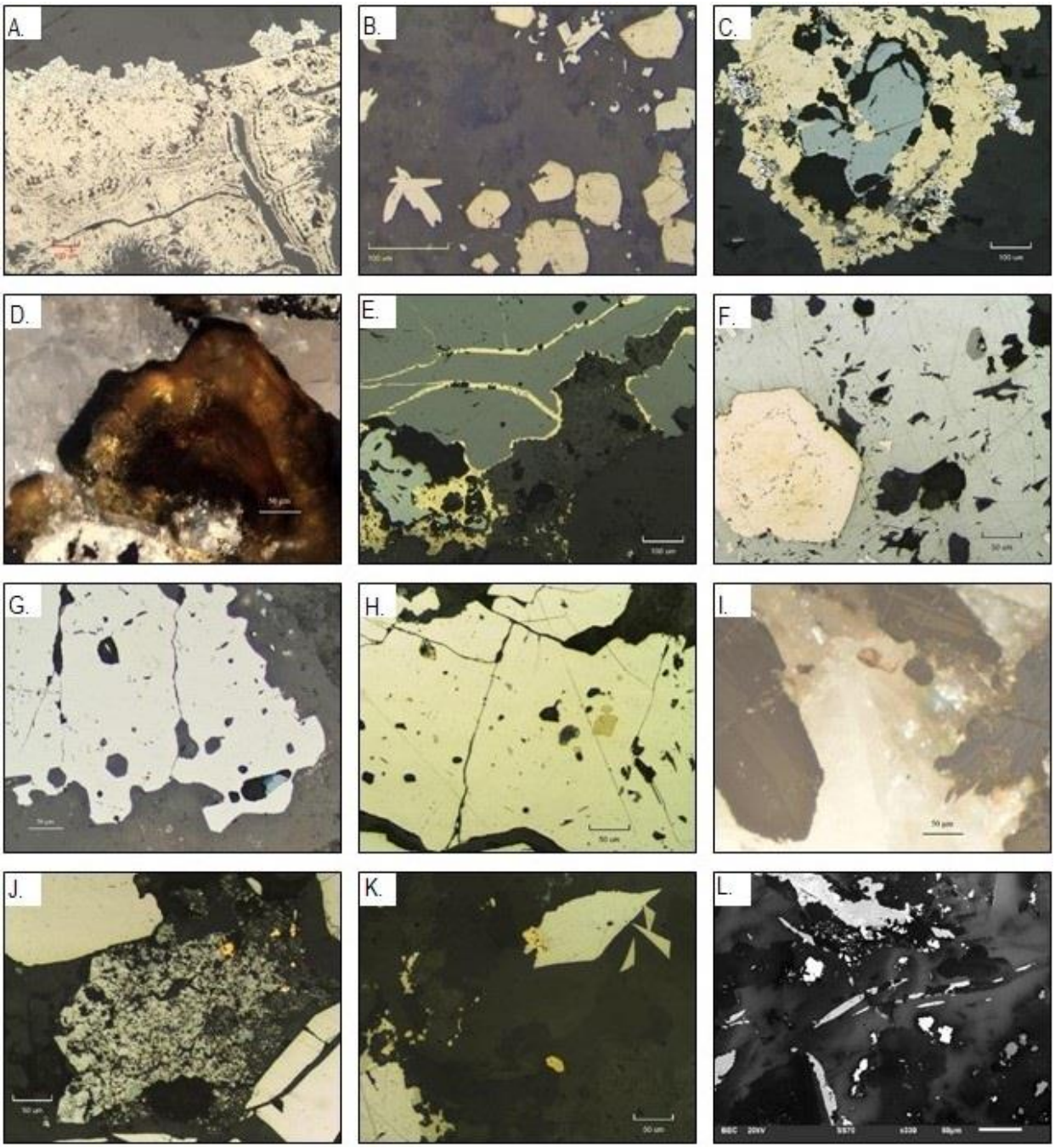

Fig. 3. Microphotographs in reflected plane polarised light, parallel Nickols (*N //*). Same conditions for all photos if not specified
A. Pyrite with colloform structure. At the upper boundary of pyrite aggregate rim of marcasite is developed (white, bluish shade, with strong anisotropy); *B*. Euhedral and semi-euhedral pyrite grains (yellowish-white) situated at the right. At the top spear-like to prismatic arsenopyrite grains (white) are observed. At the left – typical for arsenopyrite "larkspur" intergrowth; *C*. Aggregate from chalcopyrite (yellow), sphalerite (grey) and marcasite (white with bluish shade) formed around tennantite-tetrahedrite grain (light grey, in the centre); *D*. Sphalerite grain (yellowish-brown internal reflections) with zonal structure within carbonate vein. (*N+)*; *E*. Sphalerite (grey) rimmed and cross-cut by chalcopyrite (yellow). At the bottom left an aggregate from tennantite-tetrahedrite (light grey) and chalcopyrite is observed; *F*. Euhedral pyrite grain (yellow-white, at the bottom, left) located within galena (white) from the vein. At the top right single enargite grain (grey) is situated; *G*. Pyrite (white) from the veinlet contains single inclusion from tennantite-tetrahedrite (light grey) and covellite (indigo-blue with bright purple-red colors of anisotropy) – most probably formed after chalcopyrite; *H*. Pyrite aggregate (yellowish-white) contains inclusions of chalcopyrite (yellow), sphalerite (grey) and pyrrhotite (creamy, showing strong anisotropy); *I*. Prismatic bournonite-seligmanite grains with well expressed lamellar structure. Isometric galena grain was also analysed (dark to black in the centre). (*N+*); *J*. Aggregate from marcasite (greyish-white) and tennantite (grey) with five small Au grains (bright yellow) located within the interstitial space among pyrite grains; *K*. Robinsonite (?) – light grey with greenish tint – rhombic shape and 3 smaller grains with triangle contours associate with chalcopyrite (yellow). At the bottom left galena grain (white) with bournonite (light grey) at the periphery; *L*. Two jordanite grains (bright white) among dolomite (dark grey) and barite (light grey, bright). To the right from them galena crystal (white with square shape) is observed.
SEM, Backscattered electron image, COMPO regime

Table 1. *Microprobe analyses of sulfides and native gold from Milin Kamak deposit*

Mineral	Pyrite	Marcasite		Arsenopyrite			Galena		Sphalerite	Gold					
Elements (wt. %)	MK1	MK2	MK3	MK4	MK5	MK6	MK7	MK8	MK9	MK10	MK11	MK12	MK13	MK14	MK15
Fe	47.02	47.61	48.28	37.18	37.11	37.48	–	–	–	1.77	–	–	–	–	–
As	1.69	–	–	40.73	40.24	39.70	–	–	–	–	–	–	–	–	–
Pb	–	–	–	–	–	–	88.33	88.86	–	–	–	–	–	–	–
Sb	–	–	–	–	–	–	–	2.09	–	–	–	–	–	–	–
Ag	–	–	–	–	–	–	–	0.31	–	4.30	2.27	2.22	3.30	1.83	2.77
Au	–	–	–	–	–	–	–	–	–	93.93	97.73	97.78	96.7	98.17	97.23
Zn	–	–	–	–	–	–	–	–	66.32	–	–	–	–	–	–
S	52.39	52.39	51.72	22.10	22.65	22.82	11.67	11.74	33.68	–	–	–	–	–	–
Σ	101.1	100	100	100.01	100	100	100	103	100	100	100	100	100	100	100

Table 2. *Microprobe analyses of minerals from tennantite-tetrahedrite series from Milin Kamak deposit*

Mineral	Tennantite-tetrahedrite					Tennantite					Tetrahedrite			
Elements (wt. %)	MK16	MK17	MK18	MK19	MK20	MK21	MK22	MK23	MK24	MK25	MK26	MK27	MK28	MK29
Cu	41.35	40.68	42.4	41.15	42.06	45.09	37.38	37.18	42.73	46.78	38.46	37.46	38.07	28.76
Fe	0.70	1.94	–	–	–	5.62	6.68	7.09	0.45	5.70	–	2.31	1.82	–
Zn	7.58	7.50	7.06	6.73	7.10	2.28	6.45	6.54	6.73	–	6.60	6.41	5.74	6.47
Ag	–	–	–	–	–	–	–	–	–	–	1.22	1.07	0.83	14.47
As	9.87	11.62	12.59	10.22	12.05	19.36	15.05	12.81	12.64	19.57	2.75	2.98	3.22	–
Sb	14.69	11.99	11.00	15.25	11.65	–	4.31	6.73	10.96	–	26.58	25.53	26.34	27.66
S	25.81	26.28	26.95	26.65	27.15	27.66	30.13	29.65	26.46	27.95	24.38	24.24	23.90	22.64
Σ	100	100.01	100	100	100.01	100.01	100	100	99.97	100	99.99	100	99.92	100

Table 3. *Microprobe analyses of bournonite-seligmannite, jordanite, enargite, robinsonite (?) from Milin Kamak deposit*

Mineral	Bournonite-seligmannite			Bournonite			Seligmannite			Jordanite			Enargite	Robinsonite (?)	
Elements (wt. %)	MK30	MK31	MK32	MK33	MK34	MK35	MK36	MK37	MK38	MK39	MK40	MK41	MK42	MK43	MK44
Pb	48.20	48.25	46.91	48.16	47.82	46.48	50.0	48.81	50.26	68.62	69.37	69.57	–	44.46	44.29
Cu	12.38	11.84	11.86	12.39	11.97	12.17	12.75	13.04	12.99	–	–	–	49.14	–	–
As	10.30	7.72	9.25	–	–	–	15.91	15.55	14.32	7.36	7.86	7.53	18.25	4.75	5.18
Sb	12.09	15.36	14.80	23.18	23.72	24.38	3.27	4.96	5.18	9.49	8.16	8.57	–	32.99	32.84
S	17.03	16.84	17.18	16.27	16.49	19.97	18.08	17.64	17.25	14.53	14.61	14.33	32.61	17.80	17.70
Σ	100	100	100	100	100	100	100.01	100	100	100	100	100	100	100	100.01

Table 4. *Crystallochemical formulas of minerals in Tables 1–3 (only those not given in the text) calculated mainly after Chvileva et al., 1988*)

Gold (MK10)	$(Au_{0.87}Ag_{0.07}Fe_{0.06})_{1.00}$
Gold (MK11)	$(Au_{0.96}Ag_{0.04})_{1.00}$
Gold (MK12)	$(Au_{0.96}Ag_{0.04})_{1.00}$
Gold (MK13)	$(Au_{0.94}Ag_{0.06})_{1.00}$
Gold (MK14)	$(Au_{0.97}Ag_{0.03})_{1.00}$
Gold (MK15)	$(Au_{0.95}Ag_{0.05})_{1.00}$
Tennantite-tetrahedrite (MK16)	$(Cu_{10.45}Fe_{0.45}Zn_{1.60})_{12.50}(As_{2.60}Sb_{0.40})_{4.00}S_{12.82}$
Tennantite-tetrahedrite (MK17)	$(Cu_{8.60}Fe_{1.88}Zn_{1.47})_{11.95}(As_{2.52}Sb_{0.81})_{3.33}S_{13.60}$
Tennantite-tetrahedrite (MK18)	$(Cu_{10.45}Zn_{1.69})_{12.14}(As_{2.63}Sb_{1.41})_{4.04}S_{12.82}$
Tennantite-tetrahedrite (MK19)	$(Cu_{10.19}Zn_{1.62})_{11.81}(As_{2.15}Sb_{1.97})_{4.12}S_{13.08}$
Tennantite-tetrahedrite (MK20)	$(Cu_{10.24}Zn_{1.68})_{11.92}(As_{2.49}Sb_{1.48})_{3.97}S_{13.11}$
Tennantite (MK21)	$(Cu_{10.47}Fe_{1.48}Zn_{0.51})_{12.46}As_{3.80}S_{12.70}$
Tennantite (MK22)	$(Cu_{8.65}Fe_{0.27}Zn_{1.79})_{12.45}(As_{3.30}Sb_{0.51})_{3.81}S_{12.83}$
Tennantite (MK23)	$(Cu_{8.60}Fe_{1.88}Zn_{1.47})_{11.95}(As_{2.52}Sb_{0.81})_{3.33}S_{13.60}$
Tennantite (MK24)	$(Cu_{10.27}Fe_{0.20}Zn_{1.83})_{12.30}(As_{2.08}Sb_{1.91})_{3.99}S_{12.71}$
Tennantite (MK25)	$(Cu_{10.93}Fe_{1.50})_{12.33}As_{3.84}S_{12.83}$
Tetrahedrite (MK26)	$(Cu_{10.13}Zn_{1.69}\ Ag_{0.19})_{12.01}(As_{0.61}Sb_{3.65})_{4.26}S_{12.73}$
Tetrahedrite (MK27	$(Cu_{9.80}Zn_{1.63}Fe_{0.69}Ag_{0.16})_{12.28}(As_{0.65}Sb_{3.49})_{4.14}S_{12.57}$
Tetrahedrite (MK28)	$(Cu_{10.13}Zn_{1.69}Ag_{0.19})_{12.01}(As_{0.61}Sb_{3.65})_{4.26}S_{12.73}$
Ag-bearing Zn-tetrahedrite (MK29)	$(Cu_{8.11}Ag_{2.40}Zn_{1.77})_{12.28}Sb_{4.07}S_{12.65}$
Bournonite-seligmannite (MK30)	$Pb_{1.17}Cu_{0.98}(As_{0.69}Sb_{0.50})_{1.29}S_{2.67}$
Bournonite-seligmannite (MK31)	$Pb_{1.19}Cu_{0.95}(As_{0.53}Sb_{0.64})_{1.17}S_{2.69}$
Bournonite-seligmannite (MK32)	$Pb_{1.24}Cu_{1.04}Sb_{1.02}S_{2.71}$
Bournonite (MK33)	$Pb_{1.24}Cu_{1.04}Sb_{1.02}S_{2.71}$
Bournonite (MK34)	$Pb_{1.23}Cu_{1.00}Sb_{1.04}S_{2.75}$
Bournonite (MK35)	$Pb_{1.17}Cu_{1.01}Sb_{1.05}S_{2.77}$
Seligmannite (MK36)	$Pb_{1.17}Cu_{0.98}(As_{1.03}Sb_{0.05})_{1.08}S_{2.75}$
Seligmannite (MK37)	$Pb_{1.14}Cu_{1.00}(As_{1.01}Sb_{0.19})_{1.20}S_{2.70}$
Seligmannite (MK38)	$Pb_{1.19}Cu_{1.01}(As_{0.94}Sb_{0.21})_{1.15}S_{2.65}$
Jordanite (MK39)	$Pb_{14.84}(As_{4.39}Sb_{3.50})_{7.89}S_{20.31}$
Jordanite (MK40)	$Pb_{14.93}(As_{4.71}Sb_{3.00})_{7.71}S_{20.45}$
Jordanite (MK41)	$Pb_{15.16}(As_{4.51}Sb_{3.16})_{7.67}S_{20.17}$
Enargite (MK42)	$Cu_{3.04}As_{0.96}S_{4.00}$
Robinsonite (?) (MK43)	$Pb_{4.48}(Sb_{5.65}As_{1.31})_{6.96}S_{11.56}$
Robinsonite (?) (MK44)	$Pb_{4.45}(Sb_{5.62}As_{1.44})_{7.06}S_{11.50}$

Jordanite (or geocronite?) mineral phase by its composition was established in one of the polished sections. It appears as small single grains in barite-dolmite veinlet (Fig. 3.L) and as inclusions in bournonite-seligmannite. In reflected light it is a little bit brighter than the latter one with weak anisotropy. Microprobe analyses determine content of Pb close to the theoretical but also vast excess of As and Sb as well as significant deficit of S (Table 3). It is closely associated with gold, connected to late barite and carbonates.

Robinsonite (?) was observed as a single grain with rhombic shape in just one polished section, accompanied by three triangular grains close to it (Fig. 3.K). It manifests strong anisotropy with colour effects. Initially the mineral was determined by its optical characteristics as comparatively often found jamesonite $Pb_4FeSb_6S_{14}$, but lack of Fe excluded this possibility. Determined by microprobe analyses content of Pb, Sb with As admixture and S (Table 3) in such ratio defines this mineral phase as the only possible one – robinsonite $Pb_4Sb_6S_{13}$. But calculated formulas are with extremely non-stoichiometric composition – some excess of Pb, vast excess of Sb and As and a significant deficit of S.

Native gold with size of grains 5–15 μm is observed in late quartz-pyrite or carbonate-barite veinlets and in the interstitial spaces between pyrite grains in association with marcasite and sulfosalts (Fig. 3.J). Coarse gold grains (up to 140 μm) appear in groups within dolomite-barite veinlet with bournonite-seligmannite minerals in close spatial vicinity to pyrite aggregates. Gold is high probe – the content of Ag varies from 1.83 to 4.30 wt% (Table 1).

Gangue minerals

Gangue minerals are quartz, calcite, Mn-calcite, dolomite and barite. All microprobe analyses of carbonate minerals should be acccepted as qualitative, due to the carbon coating of polished sections. Qualitative microprobe analysis of dolomite (Fig. 3.L) estimates ratio of Ca:Mg:Fe approximately 5:4:1.

Barite was determined by quantitative microprobe analyses and is well distinguishable in backscattered electrons as mineral phase brighter than pyrite (Fig. 3.L). Calculated formulas are: $(Ba_{0.98}Sr_{0.06})_{1.04}S_{0.99}O_4$, $(Ba_{0.99}Sr_{0.05})_{1.04}S_{0.99}O_4$, $Ba_{1.01}S_{0.99}O_4$ and $(Ba_{0.84}Sr_{0.12})_{0.96}S_{1.02}O_4$.

Conclusions

New described minerals from Ore Zone 1 in Milin Kamak deposits are enargite, bornite, covellite, jordanite (?) and robinsonite (?). They are not mentioned in previous studies by Crummy et al. (2001), Stoykov et al. (2007), Sabeva and Mladenova (2012), and Sabeva et al. (2017).

Samples from Ore Zone 1 could be separated into two big groups. The first one comprises samples from altered, intensively pyritised volcanic rocks and in some cases with macroscopically observed quartz-pyrite veinlets. The second group represents samples from infilling ore veins with quartz-carbonate-sulfide matrix or quartz-carbonate veinlets, often containing barite and numerous sulfide ore minerals.

The first group of samples could be characterised by the following mineral composition: pyrite, marcasite, sphalerite, chalcopyrite and in less amount galena, minerals from tennantite-tetrahedrite group and arsenopyrite.

Mineral association (mainly pyrite and marcasite) of the first group of samples corresponds to the quartz-pyrite stage of mineralisation (Sabeva, Mladenova, 2012; Sabeva et al., 2017), but there is a question what is the place of found in almost all of the samples sphalerite, chalcopyrite and galena. On the other side, if this mineral association corresponds to the second quartz-polymetallic stage (Sabeva, Mladenova, 2012; Sabeva et al., 2017), presence of sphalerite, chalcopyrite and galena is similar, but there is a total lack of sulfosalts and gold is a high probe, not electrum. The second group of samples could be subdivided to two sub-groups.

The first subgroup includes samples with comparatively limited presence of sphalerite, galena and chalcopyrite. No sulfosalt minerals have been determined in these samples.

The next sub-group is characterised by the presence of sphalerite, galena, minerals from tennantite-tetrahedrite and seligmannite-bournonite series. Rare minerals are enargite, jordanite (?) and robinsonite (?). Gold grains have been determined in association with carbonate minerals and barite exactly in the samples from this sub-group. Gold grains are quite unevenly distributed with size from 8–10 μm to 140–150 μm. This mineral association could correspond to the so-called third carbonate-gold stage of mineralisation, but the main difference here is the presence of sulfosalt minerals.

Microscopically visible gold was determined in only 3 polished sections. This could be explained by its quite irregular and uneven distribution. The other factor could be the extremely small size of the grains, invisible under an optical microscope. Of course, presence of gold micro inclusions in sulfide minerals could not be excluded.

Acknowledgements. The authors should like to thank Thrace Recourses Ltd. and personaly Eng. Plamen Doychev for the support during the implementation of this study. Part of the studies is done under a project financied by Thrace Resources Ltd.

References

Chvileva, T., M. Bessmertnaia, M. Spiridonov. 1988. *Handbook for Determination of Ore Minerals in Reflected Light*. Nauka, Moscow, 508 p. (in Russian)

Crummy, J., I. Mutafchiev, I. Velinov, R. Petrunov. 2001. The Breznik epithermal Au occurrence, Western Srednegorie – Bulgaria: an ‘‘atypical”(?) low-sulphidation hydrothermal system. – In: Piestrzynski, A. et al. (Eds). *Mineral Deposits at the Beginning of the 21st Century. Balkema, Lisse*; *Proceedings 6th Biennial SGA Meeting, Cracow, Poland,* 723–726.

Dabovski, C., B. Kamenov, D. Sinnyovsky, E. Vasilev, E. Dimitrova, I. Bairaktarov. 2009. Upper Cretaceous geology. – In: Zagorchev, I., C. Dabovski, T. Nikolov (Eds). *Geology of Bulgaria. Part II. Mesozoic Geology.* Marin Drinov Academic Publishing House, Sofia, 305–611 (in Bulgarian with English abstract).

Popov, P., T. Berza, A. Grubic, I. Dimitru. 2002. Late Cretaceous Apuseni-Banat-Timok-Srednogorie (ABTS) Magmatic and Metallogenic Belt in the Carpathian-Balkan Orogen. – *Geologica Balc.*, *32*, 145–163.

Sabeva, R., V. Mladenova. 2012. Mineral composition of epithermal gold-silver deposit Milin Kamak, Western Srednogorie. – *Ann. Univ. de Sofia, Fac. gèol. et gèogr., 104*, 1-Gèol., 65–88 (in Bulgarian with English abstract).

Sabeva, R., V. Mladenova, A. Mogessie. 2017. Ore petrology, hydrothermal alteration, fluid inclusions, and sulfur stable isotopes of the Milin Kamak intermediate sulfidation epithermal Au-Ag deposit in Western Srednogorie, Bulgaria. – *Ore Geology Reviews*, *88*, 400–415.

Stoykov, S., S. Strashimirov, R. Moritz, D. Dimitrov, J. Todorov. 2007. Mineral composition of the Breznik-Bardoto Au epithermal ore occurrence (Preliminary data). – *Ann. Univ. Mining and Geol., 50*, Part I, 117–122.